Probing the Standard Model with forward proton tagging

Hilberto Silva[1,a]

[1]*Faculdade de Ciências da Universidade do Porto/Instituto de Astrofísica e Ciências do Espaço*

Project supervisor: J. Hollar
October 2020

Abstract. We conducted a feasibility study on the possibility of using the Precision Proton Spectrometer, PPS, installed on the Compact Muon Solenoid, CMS, at the Large Hadron Collider, LHC to set constrains on the cross-section of the process pp→p$\tau^+\tau^-$p. This study shows that not only is it feasible, but it can, in principle, be used not only to constrain the maximum allowed cross-section, and thus rule out some Standard Model extensions, but also to precisely measure the cross-section of this kind of interaction.

KEYWORDS: LHC, CMS, PPS, proton tagging

1 Introduction

1.1 The CMS detector.
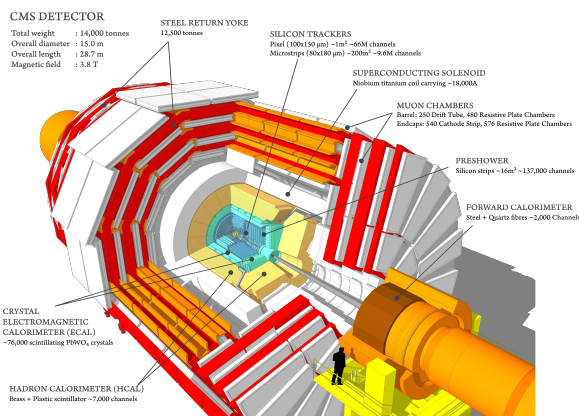
Figure 1. Overall view of the future HL-LHC CMS experiment.

The CMS detector (Compact Muon Solenoid) is one of the experiments built in the Large Hadron Collider (LHC), at CERN, one hundred meters below the surface, near the French village of Cessy. It was built to record head-on collisions of two proton beams of up to 14 TeV.

In order to fulfill the requirements of the LHC physics program, the CMS detector had to achieve certain goals, e.g. good muon identification (> 96%) and momentum resolution over a wide range of momenta and angles, good dimuon mass resolution (∼ 1% at 100 GeV), and the ability to determine unambiguously the charge of muons with $p < 1$ TeV and also, most important for this work, to efficiently trigger and offline tag τ particles. In order to do so, the CMS detector consists of a central region where the collisions occur, followed by a silicon tracker which tracks the passage of charged particles (where the curvature direction will depend on the particle charge), then an electromagnetic calorimeter, where photons and electrons typically lay their energy in the form of energy clusters and an hadronic calorimeter, where hadrons deposit their energy. After that, there is the superconducting solenoid which

produces the 3.8T magnetic field and the muon chambers, with up to four stations of gas-ionization muon detectors installed outside the solenoid and compacted between the layers of the steel return yoke (a full description can be found in [1] and [2]).
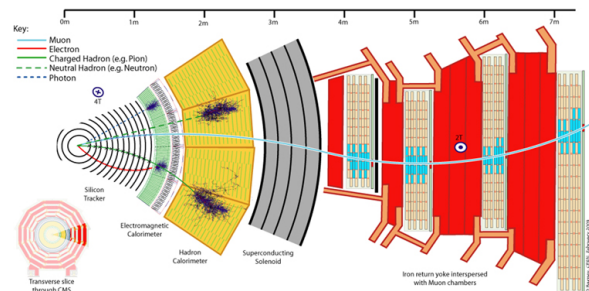
Figure 2. Schematic transverse view of the CMS detector.
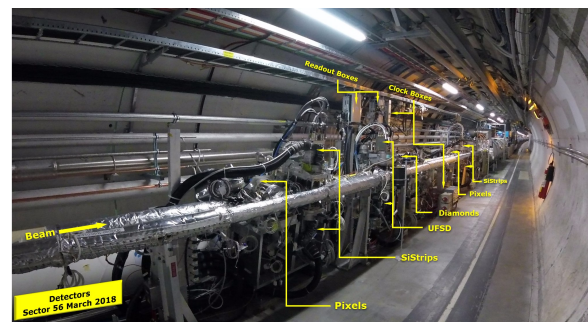
Figure 3. View inside the LHC tunnel.

1.2 The PPS detector

The Precision Proton Spectrometer is a joint CMS-TOTEM collaborations project, with the objective of adding precise tracking and timing detectors in the forward region of the CMS experiment[3].

---

[a]e-mail: hilberto.silva@astro.up.pt
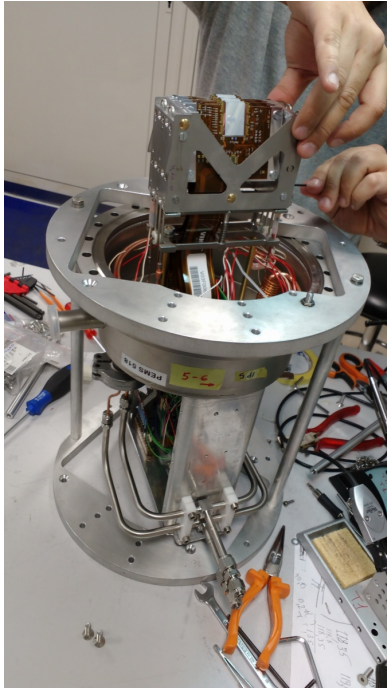
Figure 4. One of the PPS detectors.

Consisting of a silicon tracking system and a time-of-flight system, located on both sides of CMS central region, at about 210 meters from the interaction region, the PPS aims to study Central Exclusive Production in proton-proton collisions. The protons that have lost a small fraction of their momentum are bent outside the beam profile by the LHC magnets between the Interaction Point (IP) and the detector stations, and their trajectories can be measured in the CT-PPS (CMS-TOTEM PPS) detector. The detector covers an area transverse to the beam of about $4cm^2$ on each arm. It uses a total of 144 pixel readout chips. This allows a reconstruction of the mass and momentum of the centrally produced system(a full description can be found in [4]).

1.3 Scientific Rationale

The Standard Model is probably the most successful theory of Physics, with a staggering prediction ability and precise constrains, it has stood the test of time for decades. Although there have been indications that it may not be a "final theory", the Standard Model has survived increasingly demanding tests.
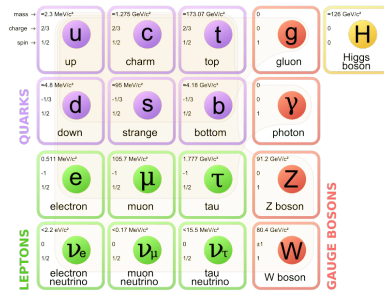
Figure 5. The fundamental particles of the Standard Model.

In the Standard Model, there are three generations of leptons, with their respective neutrinos, from the lightest (the electron, e^-) to the heaviest (the tau, τ), passing by the muon, μ and the measurement of their physical properties and their interaction with other particles, namely photons, is a crucial test to the Standard Model.

The anomalous magnetic moment was discovered in 1947 by P. Kusch and H. M. Foley. The Zeeman spectra of the gallium atom in a constant magnetic field were measured, and the gyromagnetic ratio (g value) was determined.The g value derived from the Dirac theory is exactly an integer two, and the difference between the measured g value and Dirac's exact number (2) is called the anomalous magnetic moment (g-2).

The value of the anomalous magnetic moment of leptons is highly constrained in the state-of-the-art Standard Model predictions and is one of the most precisely measured quantities that test the validity of the Standard Model. Interestingly, recent experiments have shown some tension between the theoretical and experimental value for the anomalous magnetic moment both from the electron (2.4σ) and the muon (3.7σ) [5], hinting at the possibility of a new physics beyond the Standard Model.
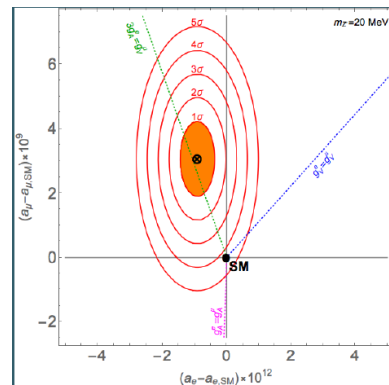
Figure 6. Experiments have shown some tensions between the SM-prediction and experimental data for the g-2 factor. (Image taken from http://resonaances.blogspot.com)

The τs are more massive and thus, in principle, more sensitive to deviations from the Standard Model, however they are more difficult to produce and to detect, due to their unstable nature.

Decay Mode	Resonance	$\mathcal{B}$ [%]
$\tau^- \to e^- \bar{\nu}_e \nu_\tau$		17.8
$\tau^- \to \mu^- \bar{\nu}_\mu \nu_\tau$		17.4
$\tau^- \to h^- \nu_\tau$		11.5
$\tau^- \to h^- \pi^0 \nu_\tau$	$\rho(770)$	26.0
$\tau^- \to h^- \pi^0 \pi^0 \nu_\tau$	$a_1(1260)$	10.8
$\tau^- \to h^- h^+ h^- \nu_\tau$	$a_1(1260)$	9.8
$\tau^- \to h^- h^+ h^- \pi^0 \nu_\tau$		4.8
Other hadronic modes		1.8
All hadronic modes		64.8

Figure 7. Modes of τ decay.

2 The experiment

In order to look for hints of new physics beyond the Standard Model, we pursue the idea that we could use the PPS and the CMS detectors to look at events where photons radiate from the beam of protons and then interact with each other to produce two opposite-sign taus, that can be reconstructed using the CMS central detectors. If a higher-than-expected occurrence of these events is observed, we may be looking at new physics[6].
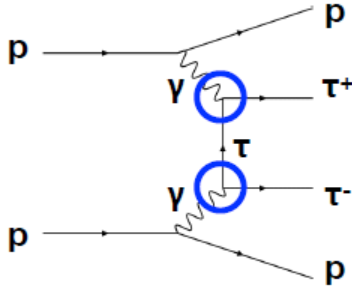
Figure 8. Feynman diagram of the interaction.

For the kind of events we will be looking at, we will need to gather the PPS data to look at the dynamics of the forward protons and look for the dynamical variables of the τs that are reconstructed by the central detectors of CMS.
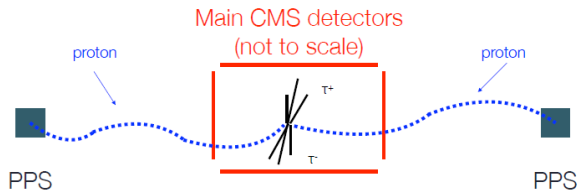
Figure 9. Schematic of the experiment.

By basic conservation of energy/momentum, the dynamics of both the τs and the protons must be correlated, considering a total energy of the collision of $\sqrt{s} = 13 TeV$, we can infer the fractional momentum loss of the protons, ξ by measuring their angle of deflection.

The mass, M, and the rapidity, Y, of the τ-pair should be given by (assuming the protons with $p_Z >> p_x, p_y$)[7]:

$$M = \sqrt{s\xi_1\xi_2} \qquad (1)$$

$$Y = \frac{1}{2}log\left(\frac{\xi_1}{\xi_2}\right) \qquad (2)$$

2.1 Background and signal

There are, of course, some difficulties in achieving this, namely the pileup, due to multiple simultaneous collisions, where the taus and the protons detected can come from different collisions (that will produce a background to the signal we are trying to detect), and the fact that the τ reconstruction can never be perfect given the fact that they always decay to, at least, one "invisible" neutrino (see fig.7).

In the range we are looking at, the most prominent and expected background comes from QCD multijets, which are responsible for the vast majority of the τ background observed, about $\sim 80\%$ [8] [9]. Almost all, about 95%, of the (misidentified) same-sign taus produced come from QCD multijets. So, in order to access the background we expect to see in the data, we will use the same-sign taus produced and later make a correction in order to more accurately predict the opposite-sign taus background. Only hadronic-modes tau-decays(in green on the table) were studied, which represent $\sim 65\%$ of all decay modes.

During the project, we explored several different data sets, of increasing difficulty, not only in order of magnitude of the data but also going from no-pileup to introducing the pileup.

In order to simulate the signal, we used CEPGEN[10] to simulate 10000 events with $\xi > 0.03$ and $p_T(\tau) > 100GeV$.

For the data, we used 6% of the data collected by PPS detectors during Run2, 2016-2018, which correspond to a luminosity of $L = 6.5 fb^{-1}$.

3 Results

3.1 Simulated data (signal)

In the following plots (fig.10-13), we used the simulated data, in order to look for the signal, imposing the following conditions:

- $\xi > 0.03$

- $p_T(\tau) > 100GeV$

- one proton detected on each arm of the PPS

- only taus produced with **opposite-signs**.

- tau_id=1 (taus pass **all** the identification tests of CMS [7])
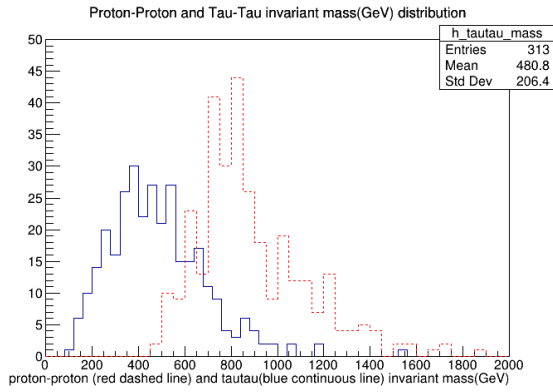
Figure 10. Distribution of the invariant mass(GeV) of the proton-proton (red dashed line) and the tau-tau (blue continuous line), data simulated with pile-up.
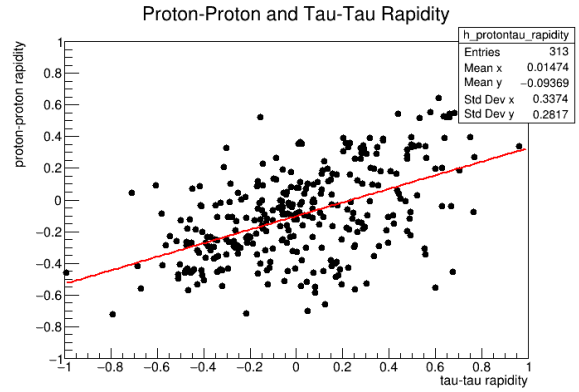
Figure 13. 2-D plot of the distribution of rapidity of the proton-proton (horizontal) and the tau-tau(vertical), data simulated with pile-up (in red the best linear fit to the distribution).
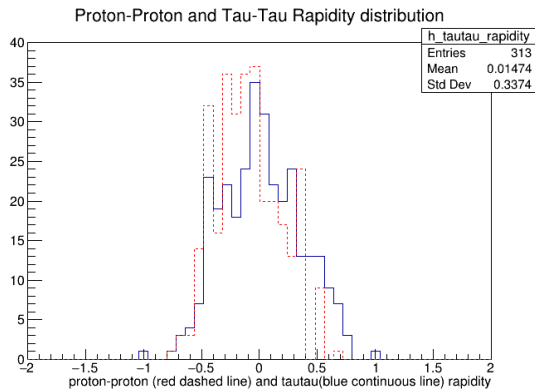
Figure 11. Distribution of rapidity of the proton-proton (red dashed line) and the tau-tau (blue continuous line), data simulated with pile-up.

3.2 PPS-CMS data (background)

In the following plots (fig. 14-17), we used the data delivered during the Round2 of the PPS experiment, in order to look for the background to the signal, imposing the same conditions used in the last section (see bullet points on section 3.1), except for the signal of the taus, that we will now accept only the same-sign pairs.
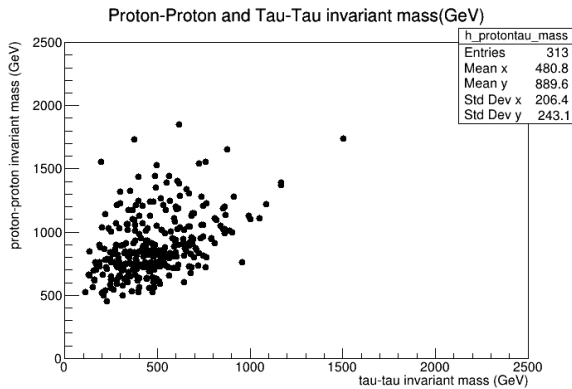
Figure 12. 2-D plot of the distribution of the invariant mass (GeV) of the proton-proton (horizontal) and the tau-tau(vertical), data simulated with pile-up.
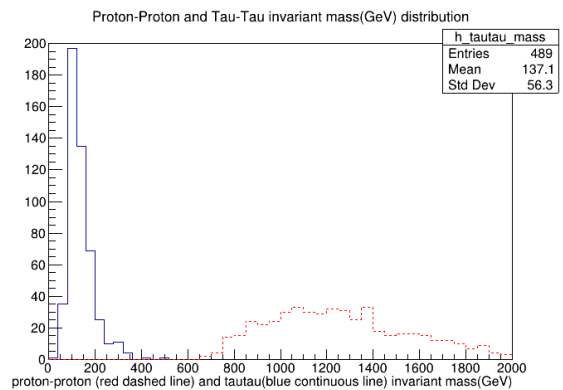
Figure 14. Distribution of invariant mass of the proton-proton (red dashed line) and the tau-tau(blue continuous line), PPS-CMS data.
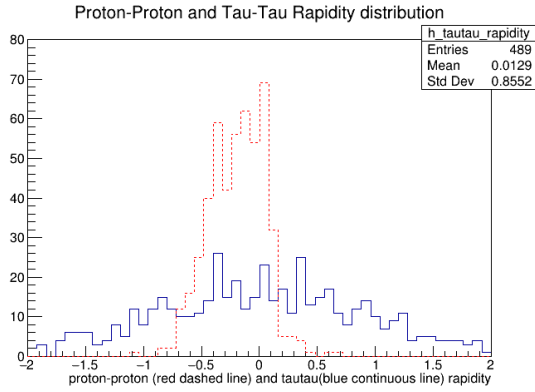
Figure 15. Distribution of rapidity of the proton-proton (red dashed line) and the tau-tau(blue continuous line), PPS-CMS data.
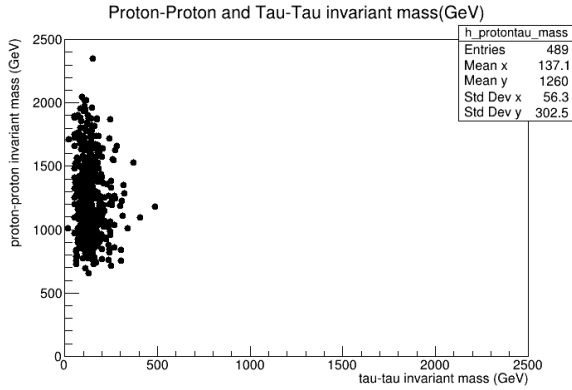
Figure 16. 2-D plot of the distribution of the invariant mass (GeV) of the proton-proton (horizontal) and the tau-tau(vertical), PPS-CMS data.
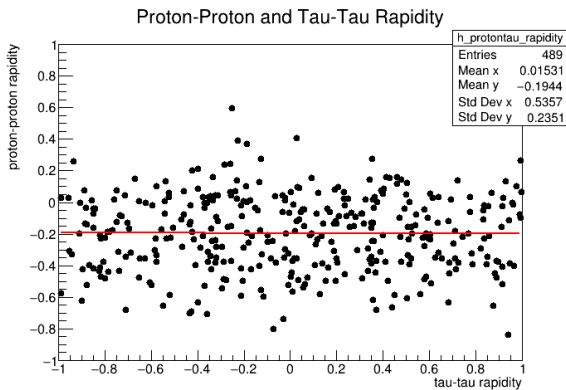
Figure 17. 2-D plot of the distribution of the rapidity of the proton-proton (horizontal) and the tau-tau(vertical), PPS-CMS data.

3.3 Data treatment

As we can see in the previous plots, there is a correlation between the dynamical variables of the proton-proton and the tau-tau(fig. 13).

In order to separate the signal and the background, we tried different cuts to the data and ponder the number of signal events and background events that made the cut. Regarding the cuts on the rapidity, we used two parallel lines to the best linear fit from fig.13:

$$pp_{rapidity} = 0.6Y + b \qquad (3)$$

where $pp_{rapidity}$ is the proton-proton rapidity, Y is the tau-tau rapidity and b is the free parameter that will take the values given on the first column of the table below. Only events between both lines were considered.

Regarding the cut on the mass, the linear cut seemed natural, so we accepted only events between

$$pp_{mass} = \tau\tau_{mass} \quad \text{and} \quad pp_{mass} = \tau\tau_{mass} + c \qquad (4)$$

where c values are given on the second column of the table below. On the last column, we can find the "figure of merit", $\frac{S}{\sqrt{B}}$, where S is the number of signal events that pass both constrains (rapidity and mass), and B are the background events that "survive" the same both constrains. Note that the values shown are not yet scaled to the luminosity (L).

b	c (GeV)	N(Signal)/√N(Background)
-0.6 / 0.4	500	218
	550	119
	600	84
	650	73.88
	700	56.57
-0.6 / 0.2	500	205
	550	112
	600	79
	650	69.7
	700	53.44
-0.4 / 0.4	500	211
	550	162.4
	600	97.96
	650	82.66
	700	62.75
-0.4 / 0.2	500	198
	550	152.5
	600	91.8
	650	77.66
	700	59

Figure 18. Table showing the different values tried for the cuts on the rapidity (first column) and the mass (second column). The values of the signal are not scaled to the luminosity(L).

To maximize the figure of merit, we used the values of the first line on the table as the cut on the mass and the rapidity, resulting in the following constrains (plots 19-22):
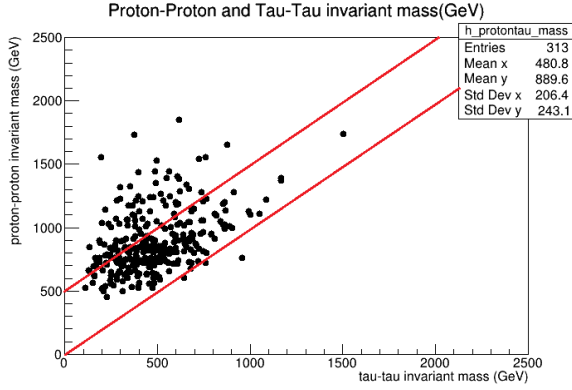
Figure 19. 2-D plot of the distribution of the invariant mass (GeV) of the proton-proton (horizontal) and the tau-tau(vertical), simulated data with pile-up, in red the cuts chosen.
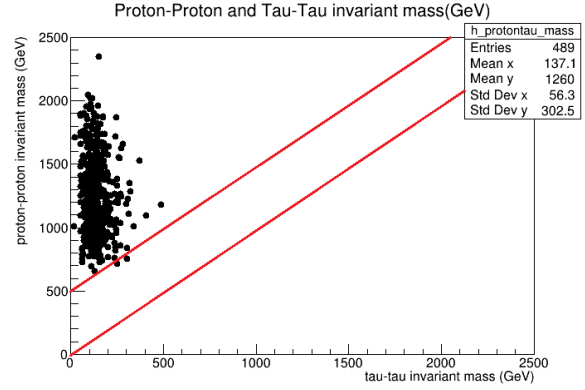
Figure 21. 2-D plot of the distribution of the mass of the proton-proton (horizontal) and the tau-tau(vertical), PPS-CMS data, in red the cut chosen.

Figure 22. 2-D plot of the distribution of the rapidity of the proton-proton (horizontal) and the tau-tau(vertical), simulated data with pile-up, in red the cut chosen (the central red line represent the best linear fit).

3.4 Background correction

As stated in 2.1, the main($\sim 80\%$) background in this process comes from QCD multijets, that are responsible for about 95% of the same-sign taus observed. We will now try to estimate, using a statistical approach, the number of expected opposite-sign taus produced by QCD multijets:

$$N(OS, Id_1) = N(SS, Id_1) \times \frac{N(OS, Id_0)}{N(SS, Id_0)} \quad (5)$$

where:

- $N(OS, Id_1)$ correspond to the number of events that produce opposite-sign (OS) taus that pass all CMS identifications tests (Id_1).

- $N(SS, Id_1)$ correspond to the number of events that produce same-sign (SS) taus that pass all CMS identifications tests (Id_1).

- $N(OS, Id_0)$ correspond to the number of events that produce opposite-sign (OS) taus that fail at least one of CMS identifications tests (Id_0).

Figure 20. 2-D plot of the distribution of the rapidity of the proton-proton (horizontal) and the tau-tau(vertical), simulated data with pile-up, in red the cut chosen (the central red line represent the best linear fit).

With these restrictions, we were able to achieve an acceptance rate, on both parameters, of $\sim 69\%$ of the signal. Applying the same cuts to the PPS-CMS data, we were able to exclude $\sim 99.7\%$ of the background, leaving only one background event that passes on both parameters.

- $N(SS, Id_0)$ correspond to the number of events that produce same-sign (SS) taus that fail at least one of CMS identifications tests (Id_0).

This correction allows us to see that, using the same-sign taus as a estimator for the real opposite-sign background underestimates the background in about 34%. So, for a 1 same-sign event background, the expected opposite-sign background to the data would be $N_{background} = 1.34$.

3.5 Prediction on the cross section

This work was done using about 6% of the total data collected during Run2 by the PPS, which amounts to a luminosity $L = 6.5 fb^{-1}$. With an acceptance rate of about $e * A \sim 2\%$, mainly due to the conditions imposed on the accepted events ($\xi > 0.03$, $p_T(\tau) > 100 GeV$, one proton on each arm and $tau\_id = 1$), we can now use Poisson statistics, without any systematics, to say that, if we observe 1 event, we can, with 95% confidence, set an upper limit of less than 4.74 events in the data. Of these, 1.34 is the expected background which leaves, with a 95% confidence level, 3.4 signal-events in the data.

We are now ready to make an upper-limit prediction on the expected cross-section for this interaction:

$$N(Signal) = (e \times A) \times L \times \sigma \qquad (6)$$

solving for σ:

$$\sigma = \frac{N(Signal)}{(e \times A) \times L} \qquad (7)$$

Substituting $e \times A = 0.02$, $L = 6.5 fb^{-1}$ and $N(Signal) = 3.4$, we get, with a 95% confidence level, an upper-limit prediction on the cross-section for this interaction of:

$$\sigma = 26 fb \qquad (8)$$

4 Conclusions and future prospects

This work was designed as a feasibility study on using Forward Proton tagging with the PPS-CMS, and hadronic tau decays, to constrain the cross section on the $pp \rightarrow p\tau^+\tau^- p$ events and, eventually, use it as a new way to search for Physics beyond the Standard Model.

The first step was to confirm whether the PPS proton-tagging and the CMS detector tau reconstruction would allow us to correlate the dynamic variables (mass and rapidity of the proton and the taus), this was achieved as can be seen, for instance, in fig. 20.

After that, we were ready to move to the analysis of the data, when we set some constrains of the events that were to be accepted (see bullet-points on section 3.1), this was in part why the acceptance rate ($e \times A$) was only 2% (see sect. 3.5).

In order to estimate the background expected to the data, we looked for same-sign tau production, of which about 95% are expected to come from QCD multijets,

which in turn account for 80% of the background to the interaction.

In order to separate the background from the signal, we set some constrains on the rapidity and the mass (see table). This allowed us to keep about 69% of the signal and to exclude 99.7% of the background. However, these cuts were done in a very naive manner, without a computational approach, which, I believe, could improve the numbers considerably.

After the constrains made, only 1 background event "survived" the cuts made on both the mass and the rapidity. We performed a statistical correction, using the taus that failed the CMS-id tests, to estimate the background expected from opposite-sign taus. Using same-sign taus underestimates the real background in about 34%.

With this data and results, we were able to make an upper-limit prediction on the cross-section for this interaction (within the generator-level acceptance cuts: $\xi > 0.03$ and $p_T(\tau) > 100 GeV$):

$$\sigma = 26 fb \qquad (9)$$

The Standard Model predicts, for this interaction, $\sigma = 0.16 fb$. So, this analysis, as it is, could only be used to rule out much-higher than SM predictions. However, the objective of this study was not to severely constrain deviations from the SM-predicted cross section, but to evaluate if it can be done using this method. We believe it can. In order to do so, looking at eq.7, we need to improve the method: use more data to increase the Luminosity and to better the acceptance.

In this study we used only 6% of the Run2 data from the PPS, which means $L = 6.5 fb^{-1}$, in Run3, starting in 2022, the improved PPS is expected to achieve a luminosity of $300 fb^{-1}$, 3 times the Run2 luminosity.

After Run3, the PPS will be removed to reconfigure the tunnel for the HL-LHC, the High Luminosity Large Hadron collider program.
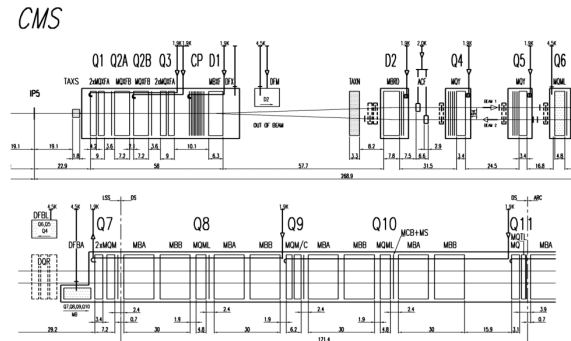
Figure 23. The CMS detector beam line at the future HL-LHC.

Within the HL-LHC program, the PPS could accumulate up to $4000 fb^{-1}$, 40 times the data collected during Run2, if a new spectrometer is installed in the beam line 23.

So, with increased data, and with improved tracking and timing detectors on the PPS[4], we could not only look

for excesses above the SM-prediction but also to precisely measure these processes.

Acknowledgements

References

[1] S. Chatrchyan et al. (CMS), JINST **3**, S08004 (2008)

[2] A.M. Sirunyan, A. Tumasyan, W. Adam, F. Ambrogi, E. Asilar, T. Bergauer, J. Brandstetter, E. Brondolin, M. Dragicevic, et al., Journal of High Energy Physics **2018** (2018)

[3] M. Albrow et al. (CMS, TOTEM) (2014)

[4] M. Gallinaro (CMS, TOTEM), AIP Conf. Proc. **1819**, 040021 (2017), 1611.07431

[5] M. Badziak, K. Sakurai, Journal of High Energy Physics **2019** (2019)

[6] S. Atağ, A. Billur, Journal of High Energy Physics **2010** (2010)

[7] A. Sirunyan, A. Tumasyan, W. Adam, F. Ambrogi, E. Asilar, T. Bergauer, J. Brandstetter, M. Dragicevic, J. Erö, A.E.D. Valle et al., Journal of Instrumentation **13**, P10005–P10005 (2018)

[8] V. Khachatryan, A.M. Sirunyan, A. Tumasyan, W. Adam, E. Asilar, T. Bergauer, J. Brandstetter, E. Brondolin, M. Dragicevic, et al., Journal of High Energy Physics **2017** (2017)

[9] A.M. Sirunyan, A. Tumasyan, W. Adam, F. Ambrogi, E. Asilar, T. Bergauer, J. Brandstetter, E. Brondolin, M. Dragicevic, et al., Journal of High Energy Physics **2018** (2018)

[10] L. Forthomme, *Cepgen - a generic central exclusive processes event generator for hadron-hadron collisions* (2018), 1808.06059